

1N-02
117410

NASA Technical Memorandum 107743

**A DETERMINATION OF THE EXTERNAL
FORCES REQUIRED TO MOVE
THE BENCHMARK ACTIVE CONTROLS
TESTING MODEL IN PURE PLUNGE
AND PURE PITCH**

Jonathan D'Cruz

(NASA-TM-107743) A DETERMINATION
OF THE EXTERNAL FORCES REQUIRED TO
MOVE THE BENCHMARK ACTIVE CONTROLS
TESTING MODEL IN PURE PLUNGE AND
PURE PITCH (NASA) 31 p

N94-12421

Unclass

G3/02 0177410

July 1993



National Aeronautics and
Space Administration

Langley Research Center
Hampton, Virginia 23681-0001

Contents

Introduction	1
Symbols	2
Equations of Motion	4
Determination of External Forces	6
Pure Plunge	7
Pure Pitch	8
Numerical Results	9
Discussion	11
Concluding Remarks	12
Acknowledgements	13
Appendix A—Format of ISAC DYN_TAPE5.DAT Files	14
Appendix B—Sample ISAC DYN_TAPE5.DAT File	15
Appendix C—FORTRAN Source Code	16
References	17
Figures	18

Introduction

As a result of a study into the ability of modern Computational Fluid Dynamics (CFD) codes to adequately analyze aeroservoelastic interactions, it was concluded that there exists a strong need for well-documented experimental data which could be used to validate and/or calibrate these codes. Although extensive data is already available in the literature, much of it is unsuitable for use in this manner. In view of this, the Structural Dynamics Division of the NASA Langley Research Center (LaRC) has initiated an experimental program in aeroelasticity. The primary aim of the program, the Benchmark Models Program (BMP), is to provide experimental data to evaluate CFD codes for aeroelastic analysis. The program also aims to provide insight into the phenomenon of unsteady flow and to provide a data base for empirical design. (See refs. 1–4.)

The BMP involves a series of aeroelastic models with different configurations to be tested in the Transonic Dynamics Tunnel (TDT) of NASA LaRC. One of these models is the Benchmark Active Controls Testing (BACT) model (ref. 1). It consists of a rigid wing of rectangular planform with a NACA 0012 profile and three control surfaces, namely, a trailing-edge control surface, a lower-surface spoiler, and an upper-surface spoiler. Figure 1 is a photograph of the BACT model, whilst figure 2 is an illustration of its planform. The model will be tested in the TDT using a flexible mount system which only allows plunging and/or pitching motion. Whilst having goals consistent with the BMP as a whole, a further important aim of the testing will be to validate analytical design tools for active control.

One data set of interest to the program would be that which results from the model oscillating sinusoidally, in turn, in pure plunge and pure pitch. Of vital interest, then, would be the forces required to cause the model to execute the prescribed plunging or pitching motion. Clearly this is because the choice of the actuation system (for example, low force-capability gas thrusters or high force-capability hydraulic jacks) depends on the force requirements. It is with the quantification of these force requirements that this report is primarily concerned.

It will be noticed that if the forces required to move the model could be determined exactly, it must mean that the aerodynamic forces acting on the model are known exactly, and hence the need would not exist to perform a test to measure these aerodynamic forces. (A major aim of the BMP is to determine the forces acting on wind tunnel models.) It should therefore be emphasized that the purpose of this report is to determine *approximately* the forces required to be applied to the model, so that the feasibility of this part of the BACT model test may be assessed.

Symbols

NOTE:(1) The term "wing" is meant to include the effect of the (fixed) trailing-edge control surface. For the purposes of this analysis, the spoilers are non-existent.

(2) The elastic axis, center of mass and mid-chord of the wing are coincident.

a	speed of sound in tunnel medium
a	n_{22}/n_{11}
b	semi-chord
b	$(\lambda_1 + \lambda_2)/n_{11}$
c	$\lambda_1 \lambda_2 / (n_{11} n_{22} - n_{12} n_{21})$
d_A	distance of F_A from mid-chord of wing
d_B	distance of F_B from mid-chord of wing
d_c	distance between trailing-edge control surface hinge line and center of mass of trailing-edge control surface
d_h	distance of trailing-edge control surface hinge line from mid-chord of wing
f	frequency
F_A	external point force acting on model at distance d_A forward of mid-chord of wing (positive up)
F_B	external point force acting on model at distance d_B aft of mid-chord of wing (positive up)
f_i	i^{th} wind-off natural frequency
$f(x)$	aerodynamic force per unit chord length
g_i	i^{th} modal damping ratio
H	hinge moment about trailing-edge control surface hinge line (positive nose-down)
i	$\sqrt{-1}$
I	moment of inertia of wing about mid-chord of wing
\mathbf{I}	identity matrix
I_ξ	moment of inertia of trailing-edge control surface about its center of mass
k	plunge stiffness of pitch and plunge mount
k	reduced frequency, $\omega b/V$
K	pitch stiffness of pitch and plunge mount
\mathbf{K}	generalized stiffness matrix
k_i	i^{th} reduced frequency
k_{ij}	ij^{th} term of \mathbf{K}
L	lift force acting through mid-chord of wing (positive up)
m	mass of wing

M	Mach number
\mathbf{M}	generalized mass matrix
m_{ij}	ij^{th} term of \mathbf{M}
m_ξ	mass of trailing-edge control surface
n_{ij}	ij^{th} element of \mathbf{M}^{-1}
P	pitching moment about mid-chord of wing (positive nose-down)
\mathbf{q}	generalized displacement vector, given by $\mathbf{z} = [y \ \theta \ \xi]^T$
\mathbf{Q}	matrix of generalized aerodynamic force coefficients
q_D	dynamic pressure, $\frac{1}{2}\rho V^2$
q_{ij}	given by $q_D(q_{ijR} + iq_{ijI})$, that is, the ij^{th} term of $q_D \mathbf{Q}$
q_{ijI}	imaginary part of ij^{th} term of \mathbf{Q}
q_{ijR}	real part of ij^{th} term of \mathbf{Q}
s_{ij}	contribution of j^{th} mode to i^{th} sensor reading
t	time
T	kinetic energy of system
U	potential energy of system
V	free-stream velocity
v_g	gust velocity (positive up)
\bar{v}_g	non-dimensional gust velocity, given by $\bar{v}_g = v_g/V$ (positive up)
x	chordwise distance from mid-chord of wing (positive aft)
y	vertical displacement of mid-chord of wing from equilibrium (positive down)
Y	amplitude of plunging motion
δW	virtual work done by aerodynamic forces
θ	pitch angle of wing from equilibrium (positive nose-up)
Θ	amplitude of pitching motion
λ	eigenvalues of $\mathbf{M}^{-1}\mathbf{K}$
λ_i	i^{th} non-zero eigenvalue of $\mathbf{M}^{-1}\mathbf{K}$
ξ	deflection of trailing-edge control surface relative to wing (positive trailing-edge down)
ρ	density of wind-tunnel medium
ω	circular frequency
ω_y	circular frequency of plunging motion
ω_θ	circular frequency of pitching motion

Equations of Motion

The equations of motion will be derived to take into account the effect of trailing edge control surface motion and vertical gusts. This is because the numerical model from which the aerodynamic forces are extracted include the forces acting on the wing due to these two phenomena. The spoilers, for the purposes of this analysis, are non-existent.

Prior to any testing, the model will be balanced so that the system center of mass coincides with the elastic axis of the mount system, which also corresponds to the mid-chord position. This decouples the plunging and pitching modes, provided the trailing-edge control surface is fixed. (Compare with ref. 4.)

For the purposes of this analysis, the effect of gravity is ignored. Although this effect is of great importance as far as the position of the trailing-edge control surface is concerned, neglecting it does not affect the results as the trailing-edge control surface is later fixed.

The equations of motion may be formulated by making use of Lagrange's equations (ref. 5). With reference to figure 3, the system kinetic energy and potential energy are respectively given by

$$T = \frac{1}{2}m\dot{y}^2 + \frac{1}{2}I\dot{\theta}^2 + \frac{1}{2}m_{\xi}\left[\dot{y} + (d_h + d_c)\dot{\theta} + d_c\dot{\xi}\right]^2 + \frac{1}{2}I_{\xi}(\dot{\theta} + \dot{\xi})^2 - \frac{1}{2}m_{\xi}\left[\dot{y} + (d_h + d_c)\dot{\theta}\right]^2 - \frac{1}{2}I_{\xi}\dot{\theta}^2 \quad \text{and} \quad (1)$$

$$U = \frac{1}{2}ky^2 + \frac{1}{2}K\theta^2. \quad (2)$$

Using Equations (1) and (2) in conjunction with Lagrange's equations gives, as the *in vacuo* equations of motion,

$$\mathbf{M}\ddot{\mathbf{q}} + \mathbf{K}\mathbf{q} = \mathbf{0}, \quad \text{where} \quad (3)$$

$$\mathbf{M} = \begin{bmatrix} m & 0 & m_{\xi}d_c \\ 0 & I & m_{\xi}(d_h + d_c)d_c + I_{\xi} \\ m_{\xi}d_c & m_{\xi}(d_h + d_c)d_c + I_{\xi} & m_{\xi}d_c^2 + I_{\xi} \end{bmatrix},$$

$$\mathbf{K} = \begin{bmatrix} k & 0 & 0 \\ 0 & K & 0 \\ 0 & 0 & 0 \end{bmatrix} \quad \text{and} \quad \mathbf{q} = \begin{bmatrix} y \\ \theta \\ \xi \end{bmatrix}.$$

It will be noted that the effect of structural damping has been neglected. This is justified by the fact that any structural damping present will be small. (Table 1 of ref. 4 quotes an experimentally measured structural damping figure of 0.0024 for both the plunge and pitch modes for a NACA 0012 aerofoil with the same mounting system.)

Now let the system be acted upon by external non-conservative forces. These forces consist of (1) the aerodynamic forces, and (2) any other external non-conservative forces. The aerodynamic forces are represented in figure 4. The virtual work done by these forces is given by

$$\begin{aligned} \delta W &= -\int_{-b}^b f(x) dx (\delta y + x \delta \theta) - \int_{d_h}^b f(x) dx (x - d_h) \delta \xi \\ &= -\delta y \int_{-b}^b f(x) dx - \delta \theta \int_{-b}^b x f(x) dx - \delta \xi \int_{d_h}^b (x - d_h) f(x) dx. \end{aligned}$$

That is,

$$\delta W = (-L) \delta y + (-P) \delta \theta + (-H) \delta \xi, \quad \text{where} \quad (4)$$

$$L = \int_{-b}^b f(x) dx,$$

$$P = \int_{-b}^b x f(x) dx, \quad \text{and}$$

$$H = \int_{d_h}^b (x - d_h) f(x) dx,$$

are the aerodynamic lift, pitching moment (about the mid-chord of the wing) and hinge moment (about the trailing-edge control surface hinge line) respectively. Hence, the equations of motion, including the aerodynamic forces, become

$$\mathbf{M} \ddot{\mathbf{q}} + \mathbf{K} \mathbf{q} + [\begin{matrix} L & P & H \end{matrix}]^T = \mathbf{0}. \quad (5)$$

Now, for *constant amplitude sinusoidal motion*, the vector $[\begin{matrix} L & P & H \end{matrix}]^T$, the generalized aerodynamic force vector, may be represented by

$$[L \ P \ H]^T = q_D Q [y \ \theta \ \xi \ \bar{v}_g]^T, \quad (6)$$

$\bar{v}_g = v_g / V$ being the vertical gust velocity, v_g , non-dimensionalized by the free-stream velocity, V , Q a matrix of generalized aerodynamic force coefficients, and q_D the dynamic pressure (ref. 6). (The contribution due to gusts is later excluded from consideration.)

Now, if, as shown in figure 5, the external point forces F_A and F_B also act on the structure, the complete equations of motion, including the effect of the external non-conservative forces, are

$$M\ddot{\mathbf{q}} + \mathbf{K}\mathbf{q} + q_D Q \begin{bmatrix} \mathbf{q} \\ \bar{v}_g \end{bmatrix} + \begin{bmatrix} 1 & 1 \\ -d_A & d_B \\ 0 & 0 \end{bmatrix} \begin{bmatrix} F_A \\ F_B \end{bmatrix} = 0. \quad (7)$$

Determination of External Forces

Having derived the equations of motion in the form of equation (7), it is then possible to perform an inversion to determine the point forces, F_A and F_B , in terms of the generalized coordinates.*

Let the ij^{th} term of the generalized mass, stiffness, and aerodynamic force coefficient matrices be given by m_{ij} , k_{ij} and $q_{ijR} + iq_{ijI}$ respectively. Setting $\xi = \bar{v}_g = 0$ (that is, fixing the trailing edge control surface and removing the effect of gusts) with

$$\left. \begin{aligned} y &= Y \sin \omega_y t \quad \text{and} \\ \theta &= \Theta \sin \omega_\theta t \end{aligned} \right\} \quad (8)$$

gives

$$\begin{aligned} & \left[-m_{11}\omega_y^2 + k_{11} + q_D(q_{11R} + iq_{11I}) \right] Y \sin \omega_y t \\ & + q_D(q_{12R} + iq_{12I}) \Theta \sin \omega_\theta t + F_A + F_B = 0, \quad \text{and} \end{aligned} \quad (9)$$

* In this sense, the problem described herein is a linear *Inverse Problem*, since the unknown input to a known system with a known response to this input is sought. In fact, the problem falls into the category of the *Reconstruction Problem* (ref. 7), or, more precisely, the *Force Identification* problem.

$$q_D(q_{21R} + iq_{21I})Y \sin \omega_y t + \left[-m_{22}\omega_\theta^2 + k_{22} + q_D(q_{22R} + iq_{22I}) \right] \Theta \sin \omega_\theta t - F_A d_A + F_B d_B = 0. \quad (10)$$

as the equations of motion, in which plunging and pitching motion occur with amplitudes of Y and Θ , and with circular frequencies of ω_y and ω_θ respectively (t = time).^{*} Solving equations (9) and (10) simultaneously for F_A and F_B gives

$$F_A = \frac{-d_B}{d_A + d_B} \left[\left(-m_{11}\omega_y^2 + k_{11} + q_{11} - \frac{1}{d_B} q_{21} \right) Y \sin \omega_y t + \left(\frac{1}{d_B} m_{22}\omega_\theta^2 + q_{12} - \frac{1}{d_B} k_{22} - \frac{1}{d_B} q_{22} \right) \Theta \sin \omega_\theta t \right], \text{ and} \quad (11)$$

$$F_B = \frac{-d_A}{d_A + d_B} \left[\left(-m_{11}\omega_y^2 + k_{11} + q_{11} + \frac{1}{d_A} q_{21} \right) Y \sin \omega_y t + \left(-\frac{1}{d_A} m_{22}\omega_\theta^2 + q_{12} + \frac{1}{d_A} k_{22} + \frac{1}{d_A} q_{22} \right) \Theta \sin \omega_\theta t \right], \quad (12)$$

where $q_{ij} = q_D(q_{ijR} + iq_{ijI})$, namely, the ij^{th} term of the matrix of generalized aerodynamic force coefficients \mathbf{Q} , multiplied by the dynamic pressure q_D . The point forces, F_A and F_B , required for the model to execute *pure* plunging and *pure* pitching motion may then be easily determined as follows.

Pure Plunge

If the model executes pure plunging motion, the motion of the model as a function of time may be described by the equations

$$\left. \begin{aligned} y &= Y \sin \omega_y t \quad \text{and} \\ \theta &= 0. \end{aligned} \right\} \quad (13)$$

Thus, $\Theta = 0$ is substituted into equations (11) and (12) to yield

^{*} The amplitudes may be complex to represent arbitrary phase differences between the plunging and pitching motions.

$$F_A = \frac{-d_B Y}{d_A + d_B} \left[\left(-m_{11} \omega_y^2 + k_{11} + q_D q_{11R} - \frac{1}{d_B} q_D q_{21R} \right) + i \left(q_D q_{11I} - \frac{1}{d_B} q_D q_{21I} \right) \right] \sin \omega_y t, \text{ and} \quad (14)$$

$$F_B = \frac{-d_A Y}{d_A + d_B} \left[\left(-m_{11} \omega_y^2 + k_{11} + q_D q_{11R} + \frac{1}{d_A} q_D q_{21R} \right) + i \left(q_D q_{11I} + \frac{1}{d_A} q_D q_{21I} \right) \right] \sin \omega_y t \quad (15)$$

as the forces required for the model to execute pure sinusoidal plunging motion.

Pure Pitch

Similarly, if the model executes pure pitching motion, the motion of the model may be described by

$$\left. \begin{aligned} y &= 0 \text{ and} \\ \theta &= \Theta \sin \omega_\theta t. \end{aligned} \right\} \quad (16)$$

Hence, $Y = 0$ is substituted into equations (11) and (12) to give

$$F_A = \frac{-d_B \Theta}{d_A + d_B} \left[\left(\frac{1}{d_B} m_{22} \omega_\theta^2 + q_D q_{12R} - \frac{1}{d_B} k_{22} - \frac{1}{d_B} q_D q_{22R} \right) + i \left(q_D q_{12I} - \frac{1}{d_B} q_D q_{22I} \right) \right] \sin \omega_\theta t, \text{ and} \quad (17)$$

$$F_B = \frac{-d_A \Theta}{d_A + d_B} \left[\left(-\frac{1}{d_A} m_{22} \omega_\theta^2 + q_D q_{12R} + \frac{1}{d_A} k_{22} + \frac{1}{d_A} q_D q_{22R} \right) + i \left(q_D q_{12I} + \frac{1}{d_A} q_D q_{22I} \right) \right] \sin \omega_\theta t \quad (18)$$

as the forces required for the model to execute pure sinusoidal pitching motion.

Numerical Results

With the aid of equations (14), (15), (17) and (18), the magnitudes (per unit of plunge or pitch amplitude) and phases (relative to the motion) of the forces required to cause the model to execute each of the two types of motion may be determined. The numerical values of the various terms in these equations may be determined as described below.

The Interaction of Structures, Aerodynamics, and Controls (ISAC) computer program (ref. 8) was previously used to perform an aeroservoelastic analysis of the BACT model without spoilers. It is from the results of this analysis that the majority of the numerical values required are obtained.

It should be noted that the ISAC numerical model is three-dimensional as far as the aerodynamics are concerned (that is, there is a spanwise and chordwise distribution of aerodynamic forces). This three-dimensional model is reduced to a two-dimensional one by making use of the generalized aerodynamic force coefficient matrix, Q , which contains the forces (normalized by the dynamic pressure q_D) acting on the two-dimensional model described herein due to changes in the coordinates y , θ , ξ and \bar{v}_g used to quantify this two-dimensional model.

Appendix A contains a listing of the ISAC output file DYN_TAPE5.DAT for a Mach number, M , of 0.78. The format of this file is illustrated in appendix B. As may be seen, the generalized stiffness matrix is not explicitly given. This matrix may be determined from the generalized mass matrix and the natural frequencies by the following method.

Let λ represent the eigenvalues of $M^{-1}K$, and hence the square of the natural frequencies (in rad s⁻¹) of the undamped system described by equation (8). Then, $\det(M^{-1}K - \lambda I) = 0$, or

$$\det \begin{bmatrix} n_{11}k - \lambda & n_{12}K & 0 \\ n_{21}k & n_{22}K - \lambda & 0 \\ n_{31}k & n_{32}K & -\lambda \end{bmatrix} = 0, \quad (19)$$

where n_{ij} is the ij^{th} element of M^{-1} , which in turn leads to

$$\lambda \left[\lambda^2 - (n_{11}k + n_{22}K)\lambda + (n_{11}n_{22} - n_{12}n_{21})kK \right] = 0. \quad (20)$$

If 0, λ_1 and λ_2 are the eigenvalues,

$$\lambda^2 - (n_{11}k + n_{22}K)\lambda + (n_{11}n_{22} - n_{12}n_{21})kK = \lambda^2 - (\lambda_1 + \lambda_2)\lambda + \lambda_1\lambda_2. \quad (21)$$

Equating coefficients and solving for k and K gives

$$k = \frac{b \pm \sqrt{b^2 - 4ac}}{2} \quad \text{and} \quad K = \frac{c}{k}, \quad (22)$$

where $a = n_{22} / n_{11}$, $b = (\lambda_1 + \lambda_2) / n_{11}$ and $c = \lambda_1 \lambda_2 / (n_{11} n_{22} - n_{12} n_{21})$. As may be seen from appendix A, the ISAC model has plunge and pitch natural frequencies of 3.40 Hz and 5.16 Hz respectively. Thus, set $\lambda_1 = (3.40 \times 2\pi)^2$ and $\lambda_2 = (5.16 \times 2\pi)^2$ (rad² s⁻²), and then compute M^{-1} to obtain

$$k = 216.459, 498.555 \text{ lb in}^{-1} \quad \text{and} \\ K = 33008.2, 14331.3 \text{ in-lb rad}^{-1}.$$

An examination of the eigenvectors of $M^{-1}K$ for each solution pair (k, K) (see fig. 6 for a diagrammatic representation of these eigenvectors, or, alternatively, the mode shapes of the system) reveals that the solution pair $(k = 216.459, K = 33008.2)$ results in plunge occurring before pitch, whilst the solution pair $(k = 498.555, K = 14331.3)$ results in pitch occurring before plunge. Since the plunge frequency (3.40 Hz) actually occurs before the pitch frequency (5.16 Hz),

$$k = 216.459 \text{ lb in}^{-1} \quad \text{and} \quad K = 33008.2 \text{ in-lb rad}^{-1}$$

should be chosen as the applicable stiffness values.

The generalized aerodynamic force coefficients, $q_{ijR} + iq_{ijI}$, may also be obtained from the ISAC output file of appendix A. Contained in appendix B is an explanation of the manner in which these are listed.

Finally, numerical values are required for d_A and d_B . For the purpose of this analysis, these will be taken as

$$d_A = d_B = 7 \text{ in.}$$

Using the above-mentioned numerical values, the FORTRAN program PPRFCE in appendix C was written to determine, from equations (14), (15), (17) and (18), the magnitudes (per unit of plunge or pitch amplitude) and phases (relative to the motion) of the point forces, F_A and F_B , required to constrain the model to execute each of the two types of motion (at the frequencies

corresponding to the reduced frequencies for which the generalized aerodynamic force coefficients are determined by ISAC). The tunnel medium is Freon, in which the speed of sound, $a \approx 500 \text{ ft s}^{-1}$. (This is for a 95% Freon 12/air mixture at a temperature of 530° R and a pressure of 2000 psf.) Using this value for a leads, with a model semi-chord, b , of 8 in, to the relationship between frequency, reduced frequency and Mach number illustrated in figure 7.*

Figures 8–11 contain the plotted results of four separate runs of PPRFCE for the following test conditions:

- (1) Wind-off
- (2) $M = 0.78$, $q = 100 \text{ psf}$ (below flutter)
- (3) $M = 0.78$, $q = 146 \text{ psf}$ (near[†] flutter)
- (4) $M = 0.78$, $q = 200 \text{ psf}$ (above flutter)

Discussion

The purpose of this analysis is to approximately determine the forces required to move the BACT model in pure plunge and pure pitch. The graphical data contained in figures 8–11 presents this information for various test conditions.

As expected, the wind-off behavior of the system is that of a classical undamped two degree-of-freedom system. As may be seen from figures 8(a) and 8(b), no force is theoretically required at either the plunge (3.40 Hz) or pitch (5.16 Hz) natural frequencies, to produce, respectively, pure plunging or pure pitching motion, with the forcing function shifting from being in phase with the motion to being out of phase with the motion as the frequency of excitation is increased through each natural frequency. (The lack of frequency resolution in the ISAC data used prevents this phenomenon from being exactly represented graphically in figs. 8–11. Also, note that because of the directions defined to be positive for F_A , F_B , y and θ , a 180° phase angle between F_A and F_B and the plunge coordinate y , for instance, means that F_A and F_B are actually *in phase* with y .)

* From this figure, a connection may be drawn between the forces required to move the BACT model (which, as will be seen later, can be highly frequency dependent) and the reduced frequency achievable with these forces. A great deal of emphasis is placed on this reduced frequency parameter for the BACT model test.

† The previously-determined flutter dynamic pressure at $M = 0.78$ is 146.135 psf. This was obtained by using the STABCAR module of ISAC.

For the wind-on test cases, it will be seen that the effect of aerodynamics on the forces required to produce plunging motion is small (compare fig. 8(a) to figs. 9(a), 10(a) and 11(a)). The effect of aerodynamics is, as might be expected, greater when the model executes a pitching motion (compare fig. 8(b) to figs. 9(b), 10(b) and 11(b)). This may especially be said to be so considering that the plunge forces are shown per *inch* of plunge amplitude, while the pitch forces are shown per *degree* of pitch amplitude. Because the center of pressure is closer to the point of application of F_A than it is to that of F_B , F_A is affected to a greater extent than F_B . As may be seen from figures 9(b), 10(b) and 11(b), the minima of the $|F_A|$ vs. f and $|F_B|$ vs. f curves for pitching motion now occur at different points, with the result that there is no one frequency where both the forces required to achieve pure pitching motion are theoretically zero. In fact, for the test conditions considered, the quantity $[(|F_A|, |F_B|)_{\max}]_{\min}$ is of the order of 20–30 lb per degree of pitch amplitude, and occurs when the curves intersect. In other words, the force actuators which are used to move the BACT model in pure pitch must be capable of producing 20–30 lb per degree of pitch amplitude before any *pure* pitching motion is possible. As with pure plunging motion, this minimum force requirement (which is theoretically near zero for pure plunging) occurs at a particular frequency, and increases as the amplitude of motion is increased, the frequency of motion is reduced, or, most severely, the frequency of motion is increased.

It may therefore be seen from figures 8–11 that, for the test conditions considered, only plunging motion may be achieved with negligible force. This is possible, wind-off and wind-on, only near the plunge natural frequency of 3.40 Hz. (For $M = 0.78$, this, according to fig. 7, results in a reduced frequency, $k \approx 0.035$.) As far as pure pitching is concerned, the smallest force, per degree of pitch amplitude, that will produce the motion is of the order of 20–30 lb. This occurs near $f = 4$ Hz ($k \approx 0.04$). Excitation at higher frequencies, in either plunge or pitch, requires significantly larger forces. This is attributed to the quadratic relationship between the inertial loads and the frequency of motion.

Concluding Remarks

Presented above is an approximate analytical determination of the forces required to move the BACT model in either pure plunge or pure pitch. The analysis makes use of results previously obtained from ISAC to obtain the majority of the required numerical values.

It was seen that, for the test conditions considered, only plunging motion may be achieved with negligible force. It was pointed out that this is possible, wind-off and wind-on, only near the plunge natural frequency. As far as pure pitching is concerned, the smallest force, *per degree of pitch amplitude*, that will produce the motion is of the order of 20–30 lb. This

occurs near a frequency slightly less than the pitch natural frequency. It was also pointed out that excitation at other frequencies, in either plunge or pitch, requires larger forces. This increase in the force requirement is especially significant at higher frequencies.

Acknowledgments

The author would like to thank Dr. T. E. Noll, head of the Aeroservoelasticity Branch, whose efforts have been instrumental in precipitating his attachment to NASA LaRC. He would also like to thank Ms. C. D. Wieseman, who performed the ISAC runs which generated the aeroelastic data used herein, and for the assistance provided in reconciling the ISAC model with his. In addition, of great assistance was the advice provided by Mr. M. H. Durham, Ms. S. T. Hoadley, Dr. V. Mukhopadhyay, Mr. B. Perry, III, and Mr. A. S. Pototzky. Finally, the author is grateful to Ms. A. M. Malenfant for transforming his initial handwritten document into a word-processing file, and to Mr. M. F. Riley for easing his transition to an unfamiliar computer system.

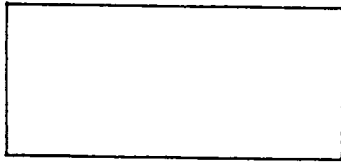
Appendix A—ISAC DYN_TAPE5.DAT File for $M = 0.78$

```

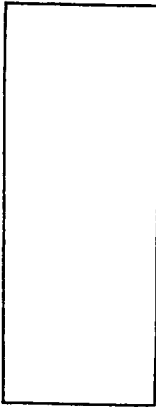
ASEB2> sh def
$2SDUCO:[DCRUZ.PAPA.RIG.MATX.ISAC_DATA]
ASEB2> ty dyn_tape5 m78.dat
0.000000 0.001000 0.005000 0.010000 0.020000 0.040000 0.060000 0.080000
0.100000 0.130000 0.160000 0.200000
0.0000000E+00 0.0000000E+00
0.0000000E+00 0.0000000E+00
0.0000000E+00 0.0000000E+00
0.0000000E+00 0.0000000E+00
0.2360745E+04 0.0000000E+00
-0.1060751E+05 0.0000000E+00
0.4733114E+02 0.0000000E+00
0.4571392E+03 0.0000000E+00
0.3123492E+03 0.0000000E+00
0.1047493E+03 0.0000000E+00
0.2360745E+04 0.0000000E+00
-0.1060751E+05 0.0000000E+00
0.4733114E+02 0.0000000E+00
0.2086285E-03 0.2950917E+00
-0.2832395E-02 -0.1325931E+01
-0.2807885E-04 0.5916387E-02
0.2360736E+04 -0.3429534E+00
-0.1060746E+05 0.2604929E+02
0.4733095E+02 0.4179317E+00
0.4571370E+03 -0.6140946E+00
0.3123663E+03 0.4820890E+01
0.1047494E+03 0.1923599E+00
0.2360725E+04 -0.5355827E+01
-0.1060739E+05 0.2987640E+02
0.4733103E+02 -0.1600142E-01
0.5209487E-02 0.1475285E+01
-0.7077803E-01 -0.6628576E+01
-0.7020520E-03 0.2958149E-01
0.2360529E+04 -0.1705897E+01
-0.1060611E+05 0.1302027E+03
0.4732767E+02 0.2089802E+01
0.4570744E+03 -0.3068403E+01
0.3127788E+03 0.2409324E+02
0.1047496E+03 0.9618196E+00
0.2360265E+04 -0.2676594E+02
-0.1060470E+05 0.1493114E+03
0.4733041E+02 -0.7988867E-01
0.2076123E-01 0.2949507E+01
-0.2827187E+00 -0.1325045E+02
-0.2809189E-02 0.5916107E-01
0.2359888E+04 -0.3357057E+01
-0.1060193E+05 0.2601355E+03
0.4731824E+02 0.4180474E+01
0.4568808E+03 -0.6124053E+01
0.3140604E+03 0.4811731E+02
0.1047505E+03 0.1923766E+01
0.2358841E+04 -0.5345046E+02
-0.1059630E+05 0.2981854E+03
0.4732938E+02 -0.1590634E+00
0.8186422E-01 0.5890697E+01
-0.1124816E+01 -0.2644846E+02
-0.1125185E-01 0.1183044E+00
0.2357406E+04 -0.6294385E+01
-0.1058562E+05 0.5182003E+03
0.4727958E+02 0.8367682E+01
0.4561239E+03 -0.1215026E+02
0.3190988E+03 0.9570166E+02
0.1047543E+03 0.3848495E+01
0.2353244E+04 -0.1062712E+03
-0.1056321E+05 0.5929800E+03
0.4732447E+02 -0.3126648E+00
0.3109684E+00 0.1172026E+02
-0.4413990E+01 -0.5250377E+02
-0.4521089E-01 0.2365471E+00
0.2348475E+04 -0.9684481E+01
-0.1052523E+05 0.1022035E+04
0.4714023E+02 0.1678198E+02
0.4533213E+03 -0.2362152E+02
0.3381290E+03 0.1876428E+03
0.1047727E+03 0.7703010E+01
0.2332174E+04 -0.2080625E+03
-0.1043750E+05 0.1161560E+04
0.4732190E+02 -0.5902881E+00
0.6501896E+00 0.1744777E+02
-0.9671860E+01 -0.7787333E+02
-0.1023003E+00 0.3549386E+00
0.2336057E+04 -0.8810893E+01
-0.1043665E+05 0.1504642E+04
0.4694393E+02 0.2526579E+02
0.4492054E+03 -0.3408465E+02
0.3670452E+03 0.2737661E+03
0.1048106E+03 0.1156420E+02
0.2300429E+04 -0.3028361E+03
-0.1024525E+05 0.1690877E+04
0.4735741E+02 -0.8263804E+00
0.1058729E+01 0.2305262E+02
-0.1667593E+02 -0.1023674E+03
-0.1829174E+00 0.4739526E+00
0.2321967E+04 -0.3495844E+01
-0.1032872E+05 0.1964955E+04
0.4671730E+02 0.3382457E+02
0.4441766E+03 -0.4346958E+02
0.4037290E+03 0.3532945E+03
0.1048725E+03 0.1542908E+02
0.2260737E+04 -0.3896496E+03
-0.1000096E+05 0.2174084E+04
0.4745755E+02 -0.1035657E+01
0.1498740E+01 0.2852791E+02
-0.2521163E+02 -0.1258700E+03
-0.2873824E+00 0.5941658E+00
0.2307489E+04 0.5982189E+01
-0.1020785E+05 0.2404241E+04
0.4647630E+02 0.4246000E+02
0.4385271E+03 -0.5180247E+02
0.4465220E+03 0.4259678E+03
0.1049593E+03 0.1929399E+02
0.2215281E+04 -0.4683183E+03
-0.9716916E+04 0.2608437E+04
0.4763315E+02 -0.1237728E+01
0.2147011E+01 0.3650571E+02
-0.4046722E+02 -0.1591340E+03
-0.4893222E+00 0.7781810E+00
0.2287047E+04 0.2702299E+02
-0.1001191E+05 0.3028612E+04
0.4611634E+02 0.5555920E+02
0.4293600E+03 -0.6247355E+02
0.5192844E+03 0.5221207E+03
0.1051388E+03 0.2508398E+02
0.2140059E+04 -0.5715457E+03
-0.9238680E+04 0.3167809E+04
0.4804606E+02 -0.1570158E+01
0.2705663E+01 0.4423395E+02
-0.5818721E+02 -0.1899548E+03
-0.7460511E+00 0.9687909E+00
0.2269994E+04 0.5468544E+02
-0.9806817E+04 0.3619389E+04
0.4579297E+02 0.6883688E+02
0.4198221E+03 -0.7121878E+02
0.5992074E+03 0.6033608E+03
0.1053749E+03 0.3085570E+02
0.2060313E+04 -0.6584796E+03
-0.8722548E+04 0.3621006E+04
0.4862977E+02 -0.1990590E+01
0.3214034E+01 0.5423873E+02
-0.8494765E+02 -0.2272798E+03
-0.1174168E+01 0.1237594E+01
0.2254662E+04 0.9873293E+02
-0.9526773E+04 0.4370152E+04
0.4548124E+02 0.8682436E+02
0.4070796E+03 -0.8045405E+02
0.7124526E+03 0.6900458E+03
0.1057707E+03 0.3850715E+02
0.1952159E+04 -0.7526026E+03
-0.8011389E+04 0.4075014E+04
0.4962676E+02 -0.2769248E+01
4.7583333E-01 0.0000000E+00 3.6212015E-03
0.0000000E+00 3.143999E+01 1.790215E-02
3.6212015E-03 1.790215E-02 8.575828E-03
3.40
5.16
0.
0. 0. 0.
-1. -5. 0.
-1. 7.15 0.
ASEB2>

```

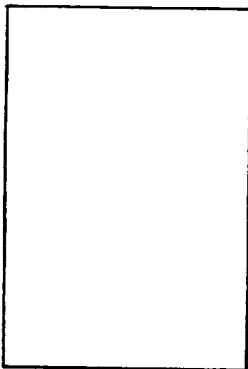
Appendix B—Format of ISAC DYN_TAPE5.DAT Files



Reduced frequencies:
 $k_i, i = 1, 2, \dots, 12$



Generalized aerodynamic forces for each reduced frequency:
 $((q_{ijR} \ q_{ijI})_k, i = 1, 2, 3), j = 1, 2, 3, 4), k = 1, 2, \dots, 12$



Generalized mass matrix:
 $(m_{ij}, j = 1, 2, 3), i = 1, 2, 3$

f_1
 f_2
 f_3

Natural frequencies (Hz): plunge, pitch, control surface

$g_1 \ g_2 \ g_3$

Modal damping ratios



Contribution of j^{th} mode to i^{th} sensor reading:
 $(s_{ij}, j = 1, 2, 3), i = 1, 2$

(Units: slinch, in, s, rad)

Appendix C—FORTRAN Source Code

```

ASEB2> sh def
$2SDUC0:[DCRUZ.PAPA_RIG.MATX]
ASEB2> ty pprfce.for
PROGRAM PPRFCE

C
C      THIS PROGRAM COMPUTES THE FORCES REQUIRED TO MOVE
C      THE BENCHMARK ACTIVE CONTROLS MODEL IN EITHER
C      PURE PLUNGE OR PURE PITCH. THE EFFECT OF
C      AERODYNAMICS IS INCLUDED BY USING DATA GENERATED
C      FROM ISAC RUNS.
C
      IMPLICIT NONE
      REAL*8 PI,M,A,RFRQ(20),QR(20,20,20),QI(20,20,20),GM(20,20),
      +NFRQ(20),D,B,M11,M22,K11,K22,OM,FAPLR,FAPLI,FBPLR,FBPLI,
      +FAPIR,FAPII,FBPIR,FBPII,FAPL,FBPL,FAPI,FBPI,FREQ,FM(20),
      +FAFBPL(20,2),FAFBPI(20,2),DUMMY,DYN,PHSEPL(20,2),PHSEPI(20,2)
      INTEGER*4 NK,I,NF,NC,NM,NG,J,K
      OPEN(UNIT=1,FILE='$2SDUC0:[DCRUZ.PAPA_RIG.MATX.ISAC_DATA]
      +DYN_TAPES_M78.DAT',STATUS='OLD',READONLY)
      OPEN(UNIT=2,FILE='FAFBM78_Q100.DAT',STATUS='UNKNOWN')

      READ IN ISAC OUTPUT:

      PI=DACOS(-1.0D0)
      M=0.78D0
      A=500.0D0*12.0D0
      NK=12
      READ(1,*) (RFRQ(I),I=1,NK)
      NF=2
      NC=1
      NM=NF+NC
      NG=1
      DYN=100.0D0/144.0D0
      DO 30 K=1,NK
        DO 20 J=1,NM+NG
          DO 10 I=1,NM
            READ(1,*) QR(I,J,K),QI(I,J,K)
            QR(I,J,K)=QR(I,J,K)*DYN
            QI(I,J,K)=QI(I,J,K)*DYN
          10 CONTINUE
        20 CONTINUE
      30 CONTINUE
      READ(1,*) ((GM(I,J),J=1,NM),I=1,NM)
      READ(1,*) (NFRQ(I),I=1,NM)

C
C      CALCULATE FA AND FB FOR PURE PLUNGE AND
C      PURE PITCH:
C
      D=7.0D0
      B=8.0D0
      M11=GM(1,1)
      M22=GM(2,2)
      K11=216.459D0
      K22=33008.2D0
      DO 90 I=1,NK
        OM=RFRQ(I)*M*A/B
        FAPLR=-(M11*OM*OM+K11*QR(1,1,I)-QR(2,1,I)/D)/2.0D0
        FAPLI=-(QI(1,1,I)-QI(2,1,I)/D)/2.0D0
        FBPLR=-(M11*OM*OM+K11*QR(1,1,I)+QR(2,1,I)/D)/2.0D0
        FBPLI=-(QI(1,1,I)+QI(2,1,I)/D)/2.0D0
        FAPIR=-(M22*OM*OM/D-K22/D+QR(1,2,I)-QR(2,2,I)/D)/2.0D0
        FAPII=-(QI(1,2,I)-QI(2,2,I)/D)/2.0D0
        FBPIR=-(M22*OM*OM/D+K22/D+QR(1,2,I)+QR(2,2,I)/D)/2.0D0
        FBPII=-(QI(1,2,I)+QI(2,2,I)/D)/2.0D0
        FAPL=DSQRT(FAPLR*FAPLR+FAPLI*FAPLI)
        FBPL=DSQRT(FBPLR*FBPLR+FBPLI*FBPLI)

        FAPI=DSQRT(FAPIR*FAPIR+FAPII*FAPII)*PI/180.0D0
        FBPI=DSQRT(FBPIR*FBPIR+FBPII*FBPII)*PI/180.0D0
        FREQ=OM/(2.0D0*PI)
        FM(I)=FREQ
        FAFBPL(I,1)=FAPL
        FAFBPL(I,2)=FBPL
        FAFBPI(I,1)=FAPI
        FAFBPI(I,2)=FBPI
        PHSEPL(I,1)=DATAN2D(FAPLI,FAPLR)
        PHSEPL(I,2)=DATAN2D(FBPLI,FBPLR)
        PHSEPI(I,1)=DATAN2D(FAPII,FAPIR)
        PHSEPI(I,2)=DATAN2D(FBPII,FBPIR)
      90 CONTINUE
      CALL MATSAV(2,'MTXFM',20,NK,1,0,FM,DUMMY,'(1P3E25.17)')
      CALL MATSAV(2,'MTXFAFBPL',20,NK,2,0,FAFBPL,DUMMY,'(1P3E25.17)')
      CALL MATSAV(2,'MTXFAFBPI',20,NK,2,0,FAFBPI,DUMMY,'(1P3E25.17)')
      CALL MATSAV(2,'MTXPHSEPL',20,NK,2,0,PHSEPL,DUMMY,'(1P3E25.17)')
      CALL MATSAV(2,'MTXPHSEPI',20,NK,2,0,PHSEPI,DUMMY,'(1P3E25.17)')
      STOP
      END
ASEB2>

```

References

- (1) Durham, M. H., Keller, F. K., Bennett, R. M., and Wieseman, C. D., *A Status Report on a Model for Benchmark Active Controls Testing*, AIAA Paper No. 91-1011, AIAA/ASME/ASCE/AHS/ASC 32nd Structures, Structural Dynamics, and Materials Conference, Baltimore, Maryland, April 8th–10th, 1991.
- (2) Bennett, R. M., Eckstrom, C. V., Rivera, J. A., Jr., Dansberry, B. E., Farmer, M. G., and Durham, M. H., *The Benchmark Aeroelastic Models Program—Description and Highlights of Initial Results*, NASA Technical Memorandum 104180, December 1991.
- (3) Dansberry, B. E., *Dynamic Characteristics of a Benchmark Models Program Supercritical Wing*, AIAA Paper No. 92-2368, AIAA/ASME/ASCE/AHS/ASC 33rd Structures, Structural Dynamics, and Materials Conference, Dallas, Texas, April 13th–15th, 1992.
- (4) Rivera, J. A., Jr., Dansberry, B. E., Bennett, R. M., Durham, M. H., and Silva, W. A., *NACA 0012 Benchmark Model Experimental Flutter Results with Unsteady Pressure Distributions*, AIAA Paper No. 92-2396, AIAA/ASME/ASCE/AHS/ASC 33rd Structures, Structural Dynamics, and Materials Conference, Dallas, Texas, April 13th–15th, 1992.
- (5) Thomson, W. T., *Theory of Vibration with Applications*, 2nd Ed., George Allen & Unwin, London, 1983, pp. 252–253.
- (6) Mukhopadhyay, V., Newsom, J. R., and Abel, I., *A Method for obtaining Reduced-Order Control Laws for High-Order Systems using Optimization Techniques*, NASA Technical Paper 1876, August 1981, pp. 3–4.
- (7) Baumeister, J., *Stable Solution of Inverse Problems*, Vieweg Advanced Lectures in Mathematics, Friedr. Vieweg & Sohn, Braunschweig/Weisbaden, 1987, p. 2.
- (8) Peele, E.; and Adams, W., *A Digital Program for Calculating the Interaction Between Flexible Structures, Unsteady Aerodynamics, and Active Controls*, NASA Technical Memorandum 80040, January 1979.

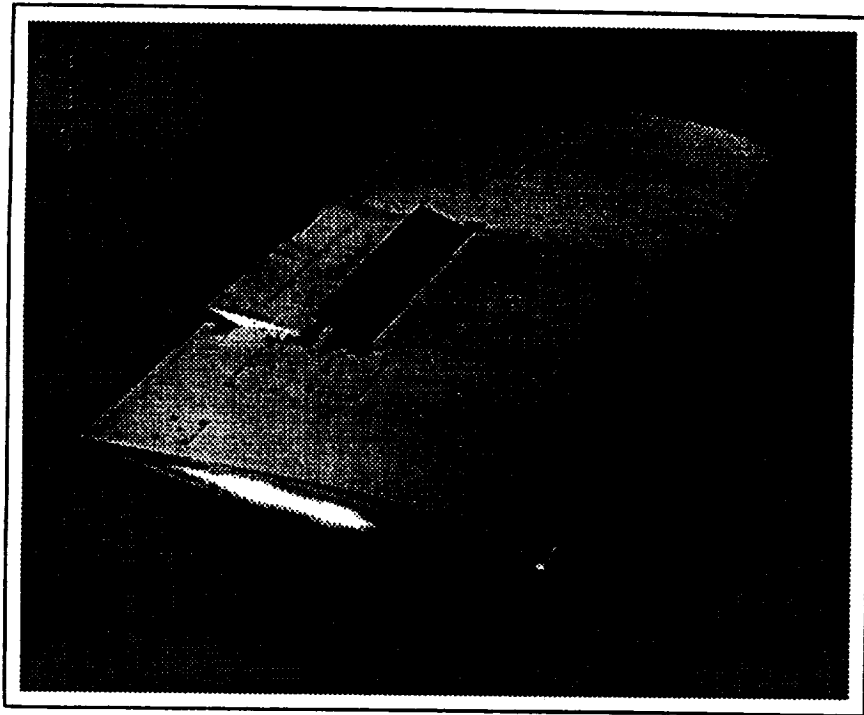


Figure 1. BACT model with deflected aileron and deployed upper-surface spoiler.

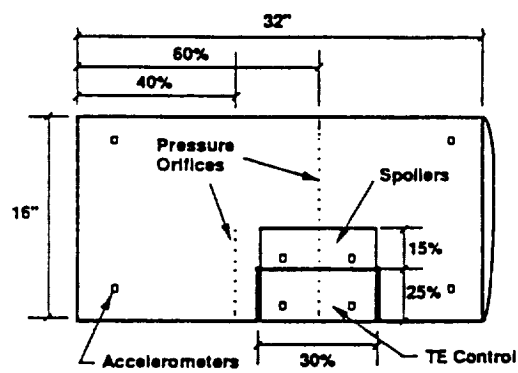


Figure 2. BACT model planform (reproduced from ref. 1, fig. 3).

- ⊗ center of mass of wing (see NOTE in Symbols section)
- × center of mass of trailing edge control surface

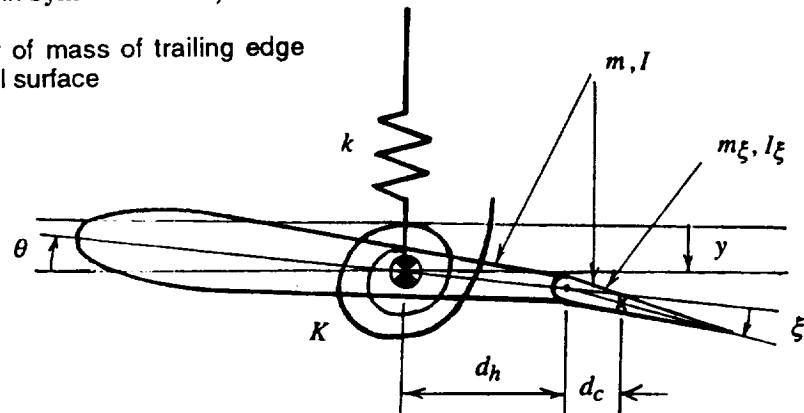


Figure 3. Model parameters and degrees of freedom.

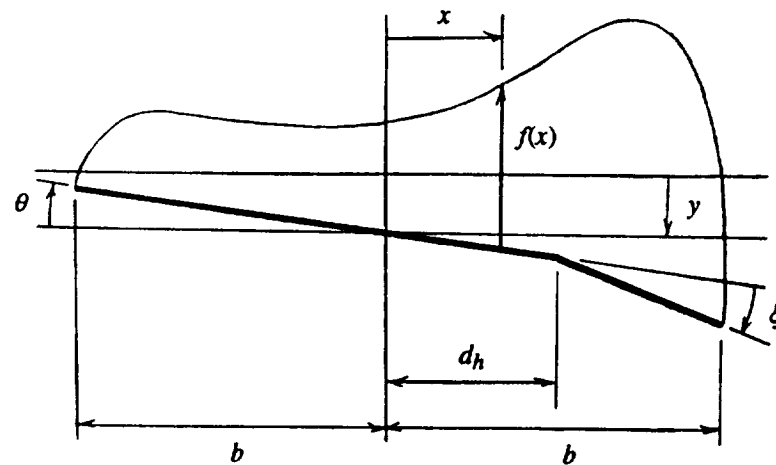


Figure 4. Aerodynamic force parameters.

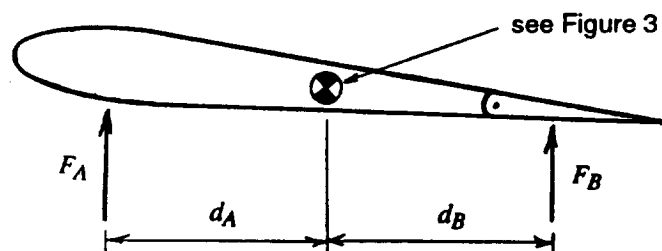


Figure 5. External applied point forces.

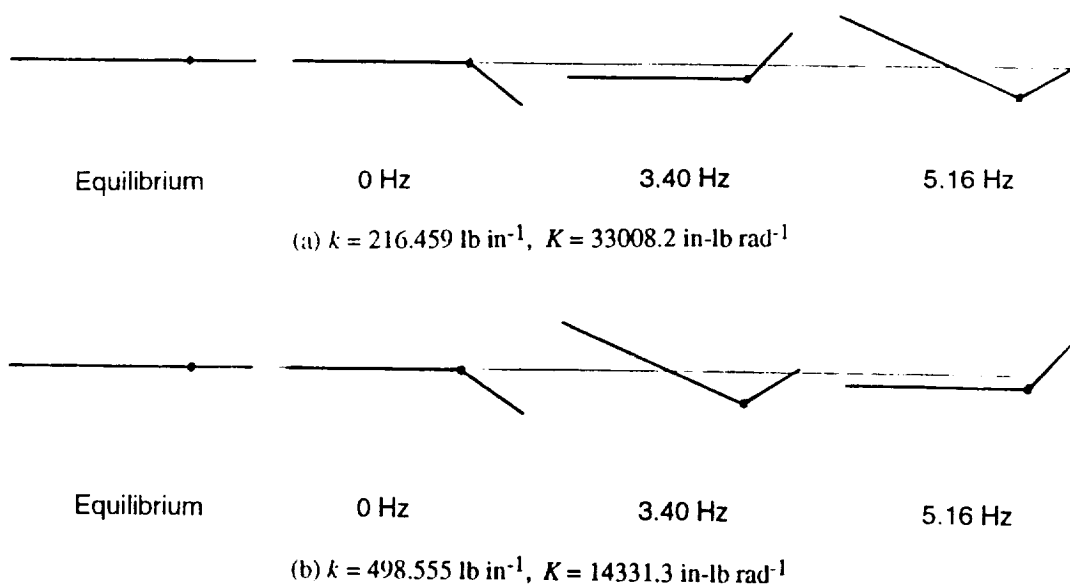


Figure 6. Mode shapes for different spring stiffnesses.

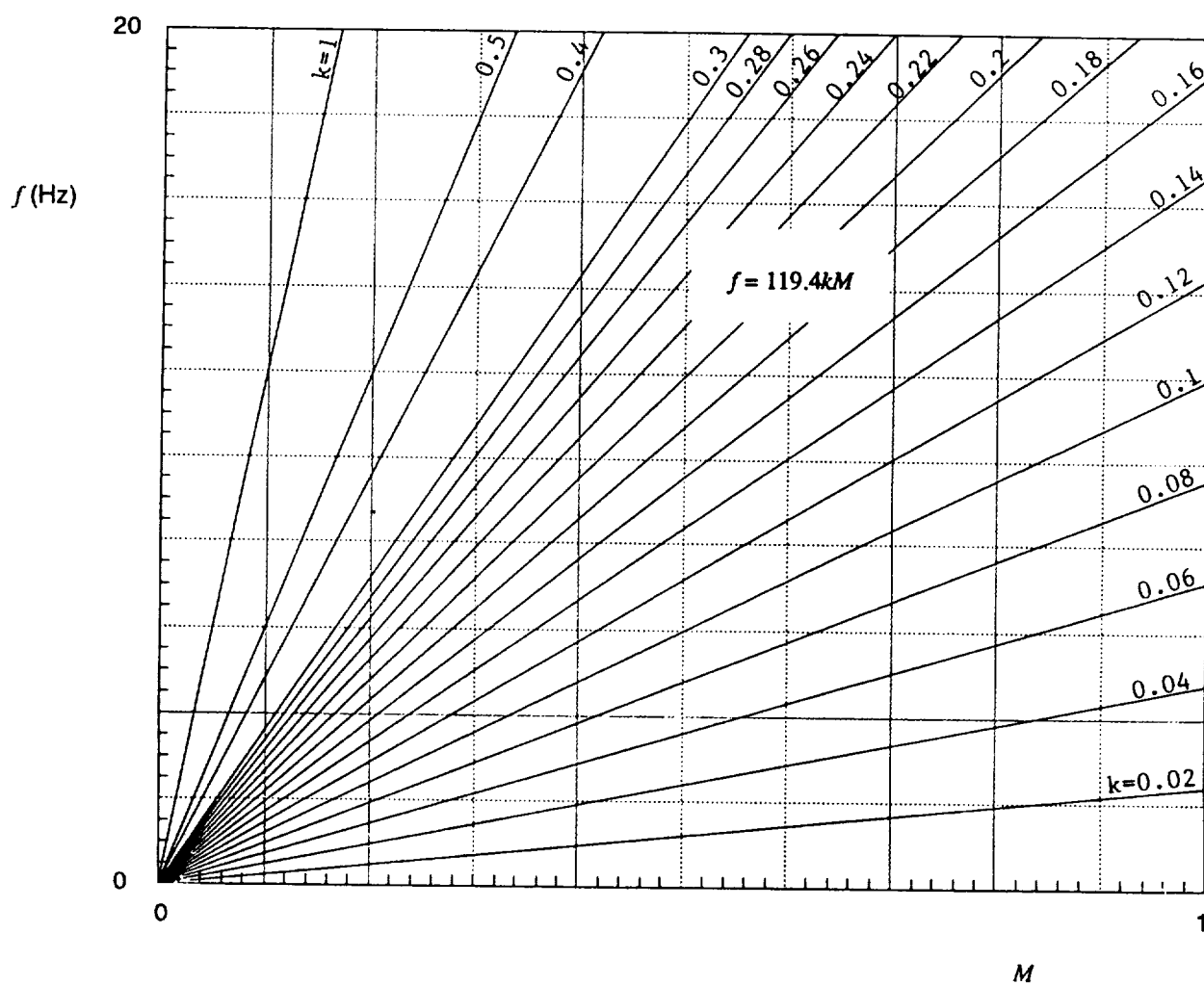


Figure 7. Relation between frequency, Mach number, and reduced frequency ($a = 500 \text{ ft s}^{-1}$).

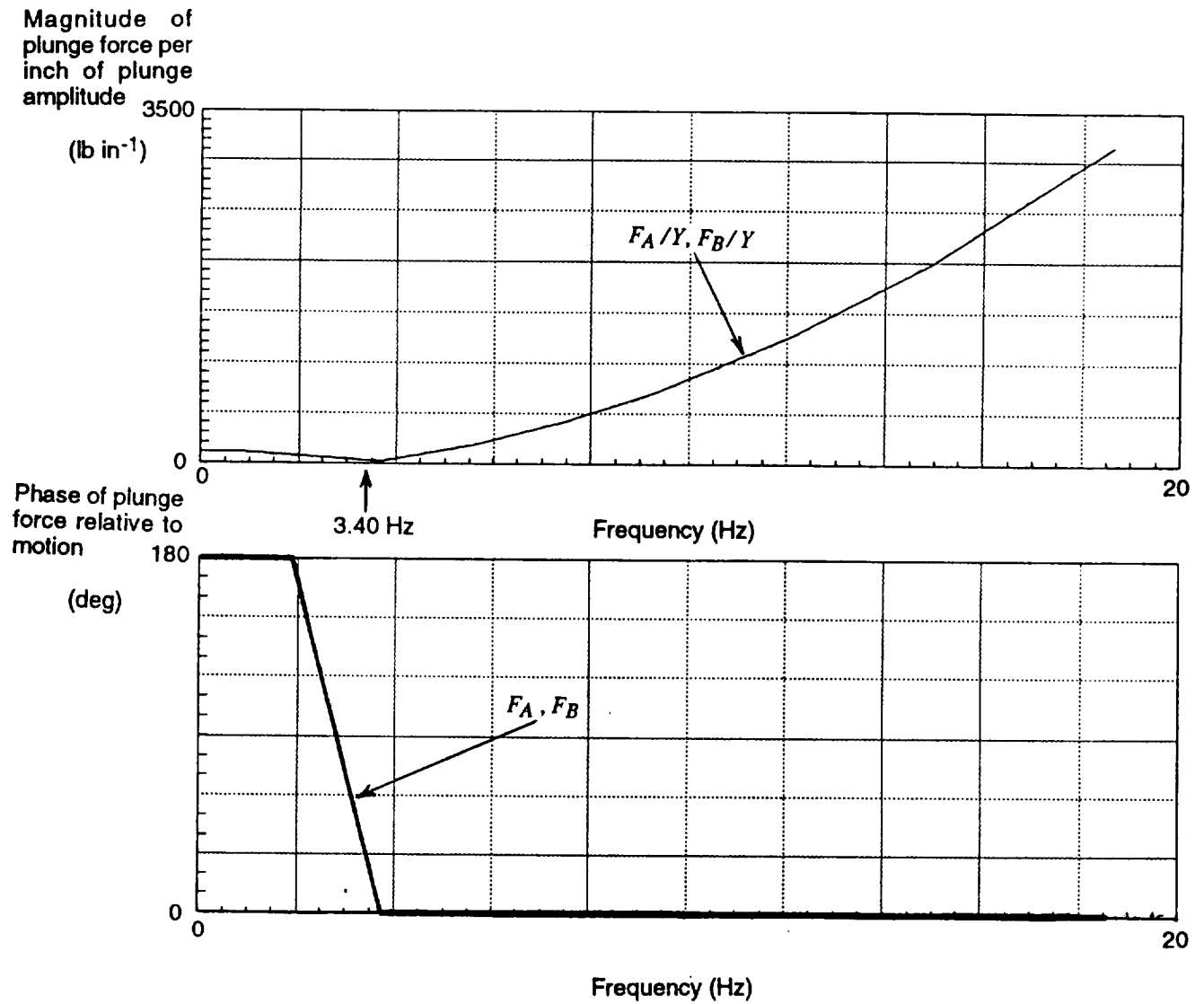


Figure 8(a). Plunge force characteristics (wind-off).

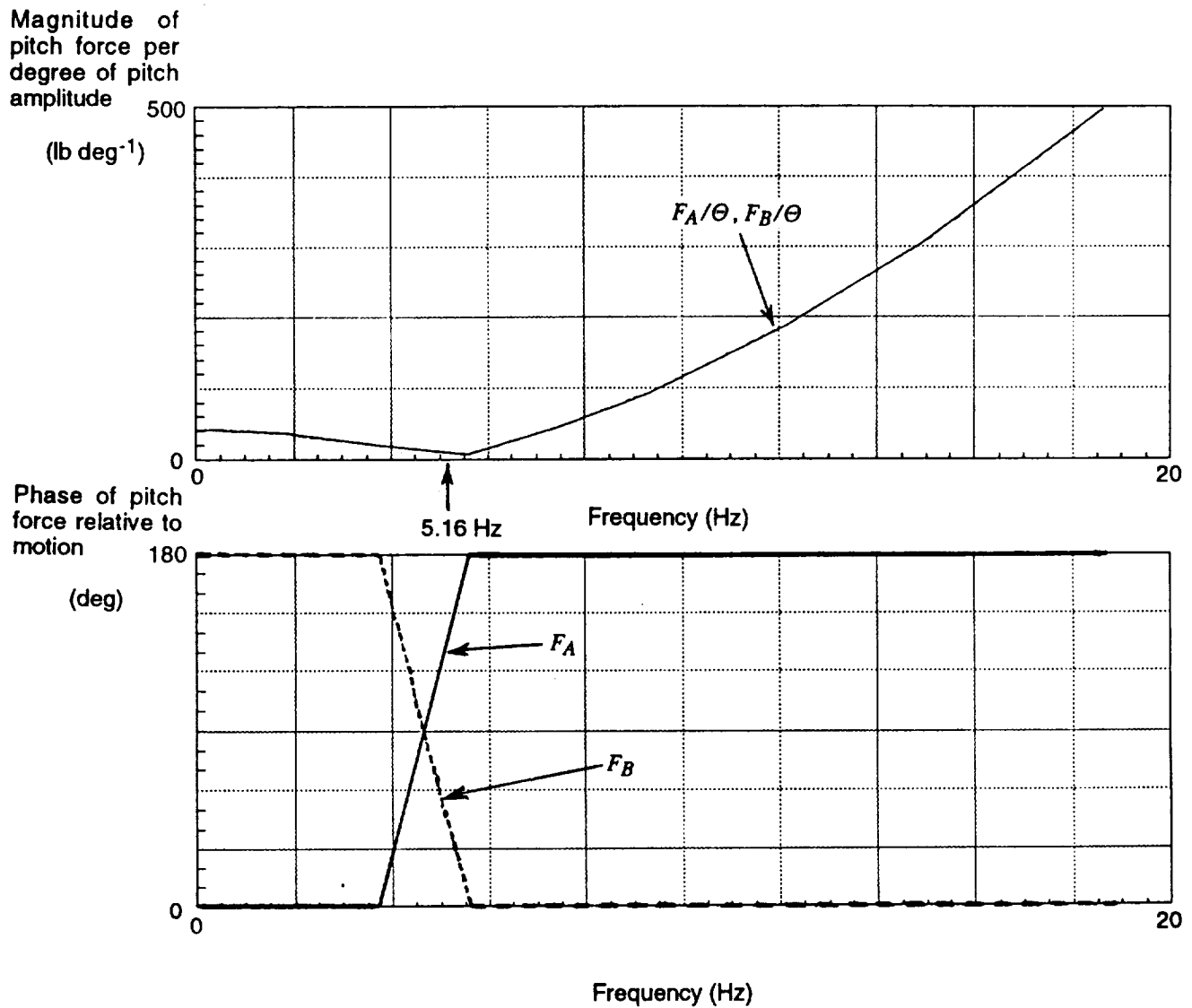


Figure 8(b). Pitch force characteristics (wind-off).

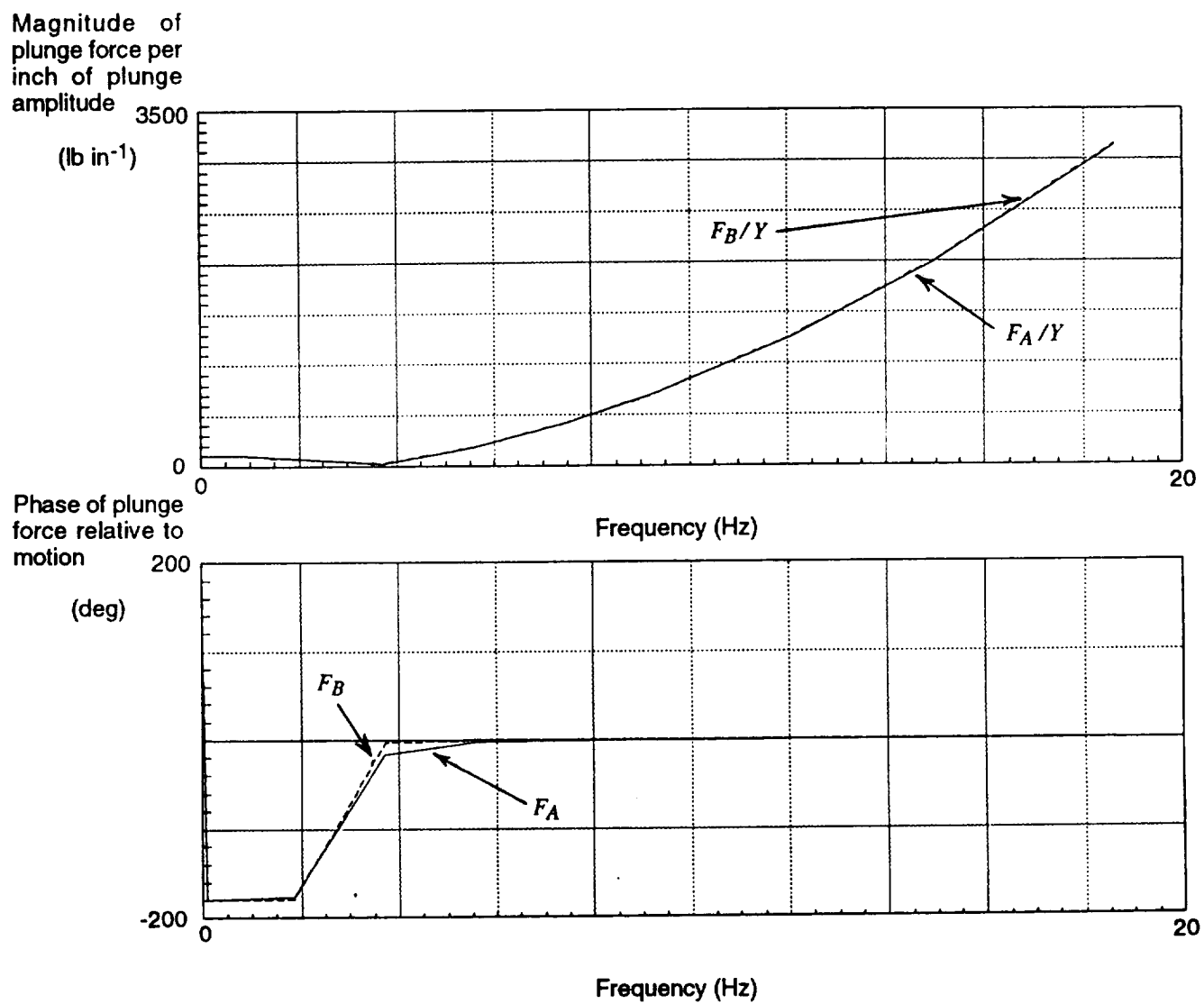


Figure 9(a). Plunge force characteristics ($M = 0.78$, $q = 100$ psf).

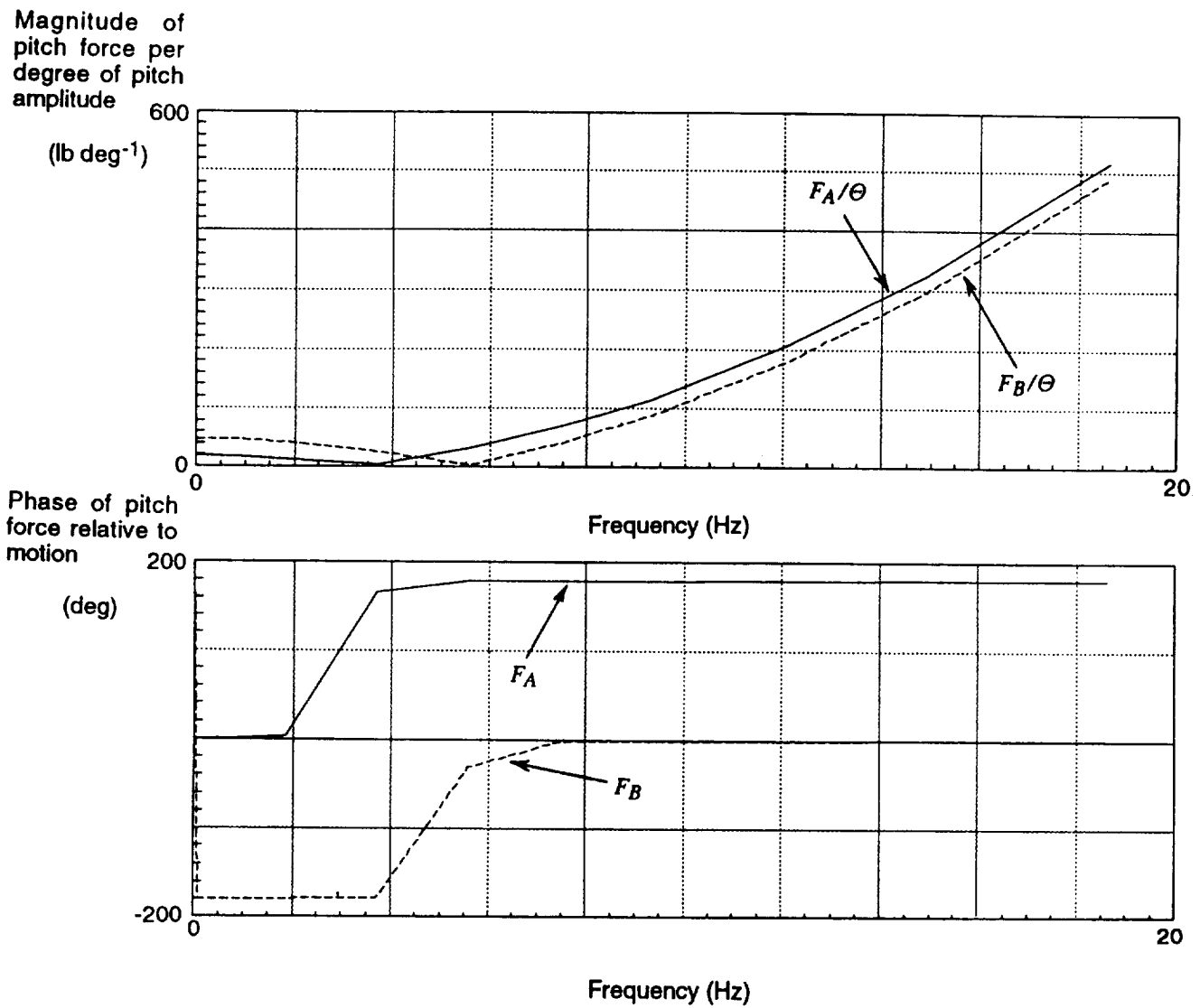


Figure 9(b). Pitch force characteristics ($M = 0.78$, $q = 100$ psf).

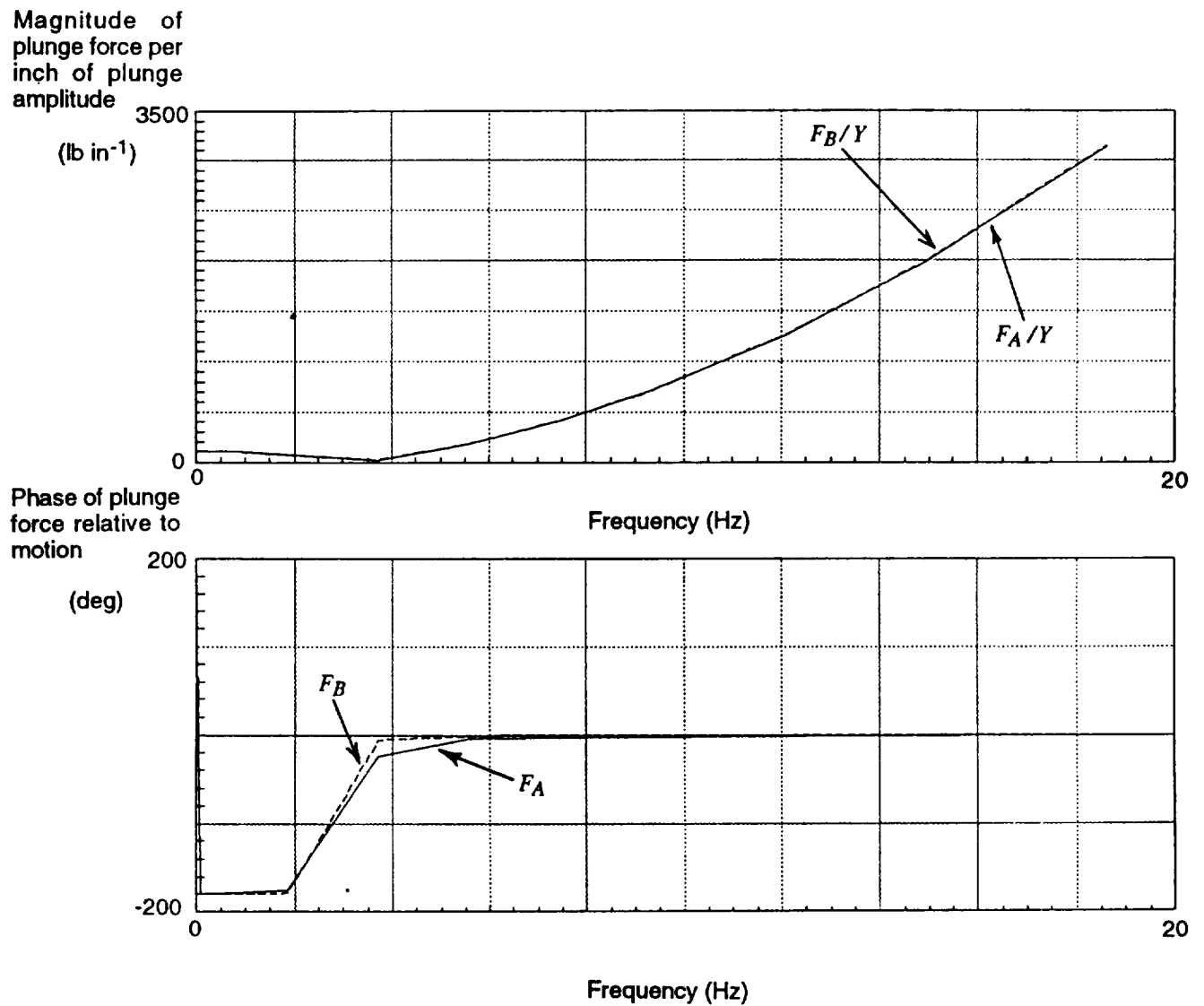


Figure 10(a). Plunge force characteristics ($M = 0.78$, $q = 146$ psf).

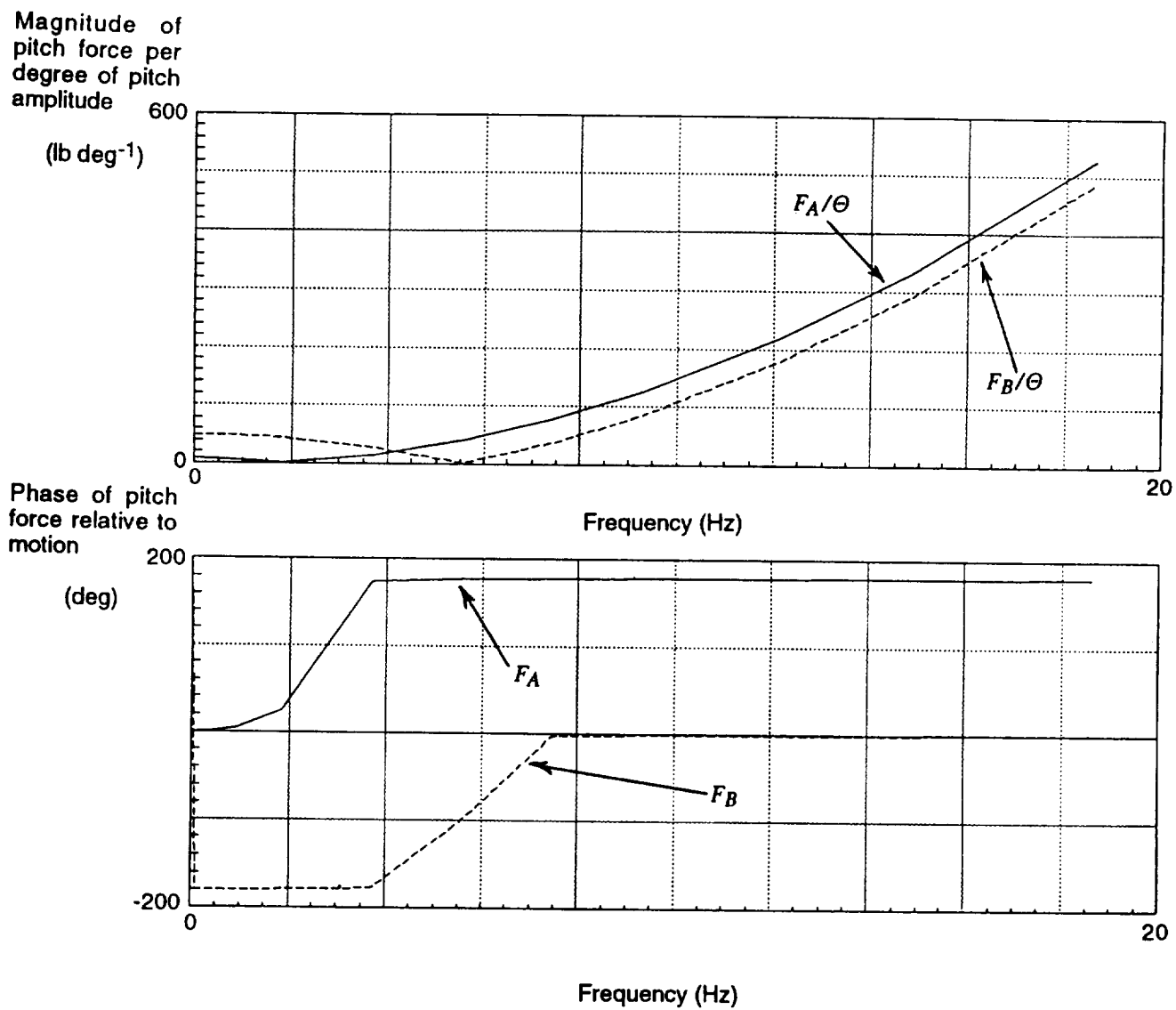


Figure 10(b). Pitch force characteristics ($M = 0.78$, $q = 146$ psf).

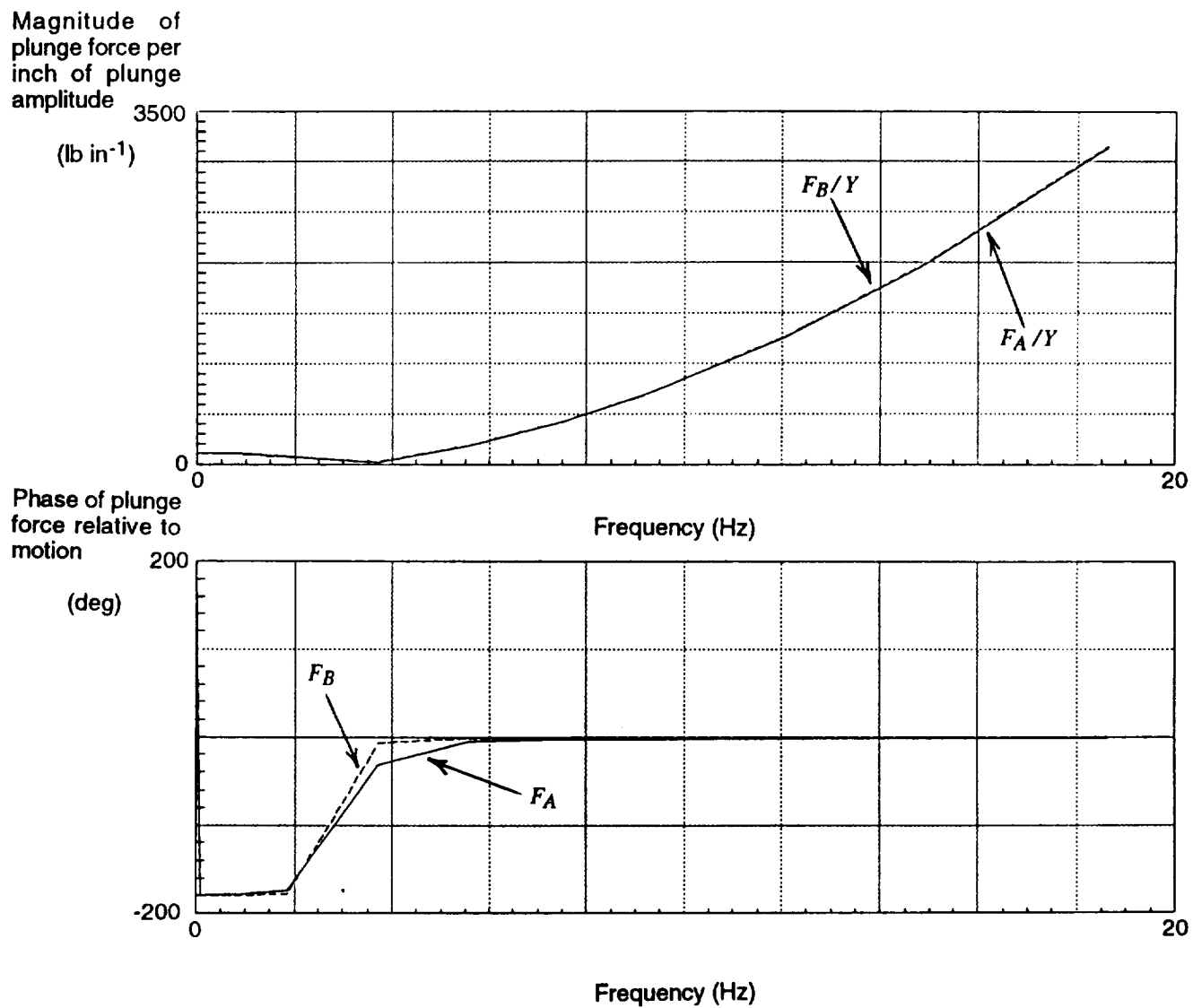


Figure 11(a). Plunge force characteristics ($M = 0.78$, $q = 200$ psf).

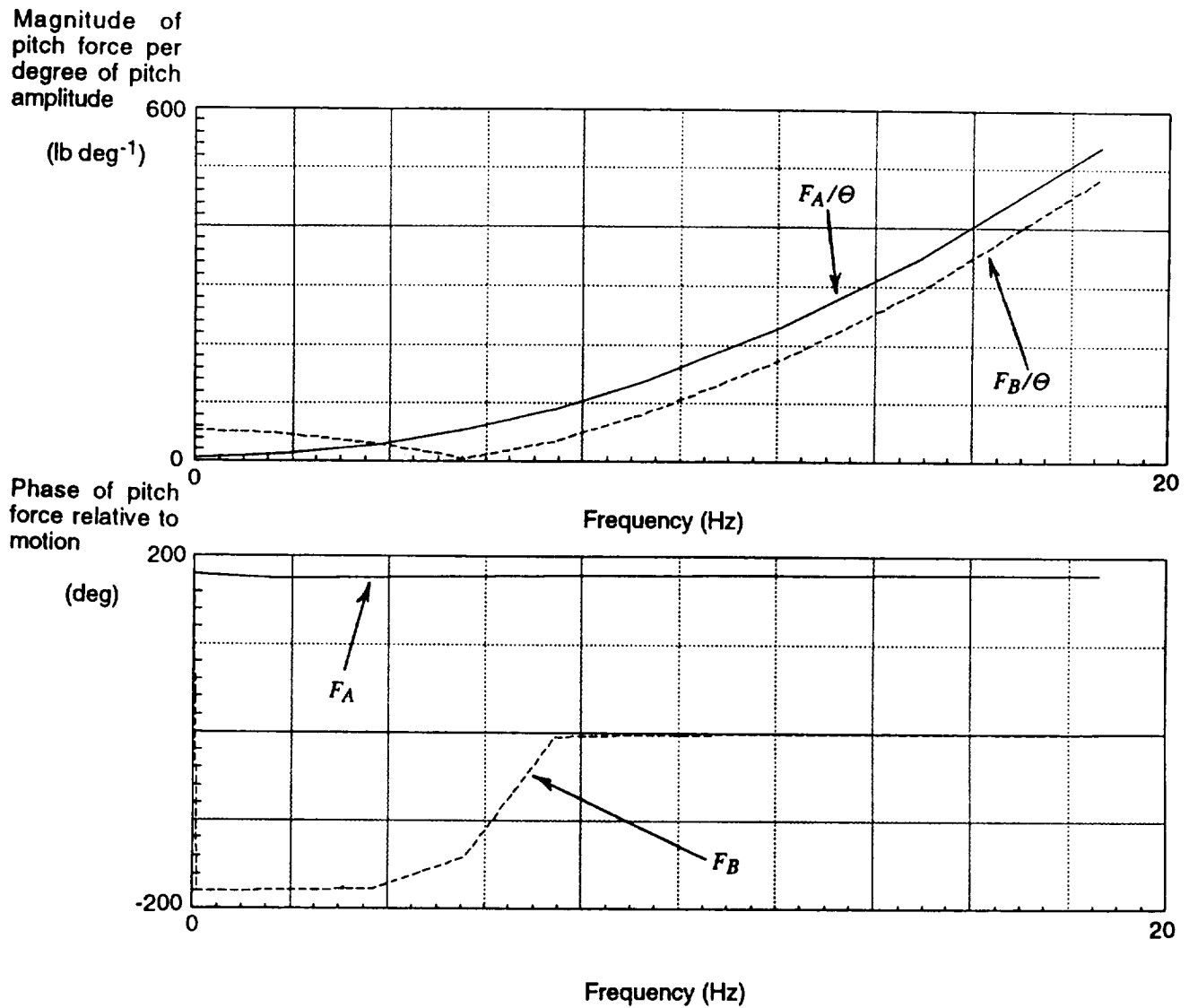


Figure 11(b). Pitch force characteristics ($M = 0.78$, $q = 200$ psf).

REPORT DOCUMENTATION PAGE			Form Approved OMB No 0704-0186	
<small>Public reporting burden for this collection of information is estimated to average 1 hour per response, including the time for reviewing instructions, searching existing data sources, gathering and maintaining the data needed, and completing and reviewing the collection of information. Send comments regarding this burden estimate or any other aspect of this collection of information, including suggestions for reducing this burden, to Washington Headquarters Services, Directorate for Information Operations and Reports, 1215 Jefferson Davis Highway, Suite 1204, Arlington, VA 22202-4302, and to the Office of Management and Budget, Paperwork Reduction Project (0704-0186), Washington, DC 20503.</small>				
1. AGENCY USE ONLY (Leave blank)		2. REPORT DATE July 1993		3. REPORT TYPE AND DATES COVERED Technical Memorandum
4. TITLE AND SUBTITLE A Determination of the External Forces Required to Move the Benchmark Active Controls Testing Model in Pure Plunge and Pure Pitch			5. FUNDING NUMBERS WU 505-63-50-15	
6. AUTHOR(S) Jonathan D'Cruz				
7. PERFORMING ORGANIZATION NAME(S) AND ADDRESS(ES) NASA Langley Research Center Hampton, VA 23681-0001			8. PERFORMING ORGANIZATION REPORT NUMBER	
9. SPONSORING / MONITORING AGENCY NAME(S) AND ADDRESS(ES) National Aeronautics and Space Administration Washington, DC 20546-0001			10. SPONSORING / MONITORING AGENCY REPORT NUMBER NASA TM-107743	
11. SUPPLEMENTARY NOTES This work was carried out while the author was attached to the Aeroservoelasticity Branch in the Structural Dynamics Division of the NASA Langley Research Center, under the auspices of The Technical Cooperation Program/Sub-Group H (Aeronautics), Technical Panel 8 (Structures and Dynamics of Aeronautical Vehicles) (TTCP/HTP-8)				
12a. DISTRIBUTION / AVAILABILITY STATEMENT Unclassified - Unlimited Subject Category 02			12b. DISTRIBUTION CODE	
13. ABSTRACT (Maximum 200 words) In view of the strong need for a well-documented set of experimental data which is suitable for the validation and/or calibration of modern Computational Fluid Dynamics codes, the Benchmark Models Program was initiated by the Structural Dynamics Division of the NASA Langley Research Center. One of the models in the program, the Benchmark Active Controls Testing Model, consists of a rigid wing of rectangular planform with a NACA 0012 profile and three control surfaces (a trailing-edge control surface, a lower-surface spoiler, and an upper-surface spoiler). The model is affixed to a flexible mount system which allows only plunging and/or pitching motion. Contained herein is an approximate analytical determination of the forces required to move this model, with its control surfaces fixed, in pure plunge and pure pitch at a number of test conditions. This provides a good indication of the type of actuator system required to generate the aerodynamic data resulting from pure plunging and pure pitching motion, in which much interest has been expressed. The analysis makes use of previously obtained numerical results.				
14. SUBJECT TERMS Benchmark Active Controls Testing Model, Benchmark Models Program, force identification, forces required to move wind-tunnel model, inverse problems, pure pitch, pure plunge, reconstruction problem			15. NUMBER OF PAGES 30	
			16. PRICE CODE A03	
17. SECURITY CLASSIFICATION OF REPORT Unclassified		18. SECURITY CLASSIFICATION OF THIS PAGE Unclassified		19. SECURITY CLASSIFICATION OF ABSTRACT
20. LIMITATION OF ABSTRACT				

